

Accurate Systemic Redshifts and Outflow Speeds for Extremely Red Quasars (ERQs)

Jarred Gillette,^{1*} Fred Hamann,¹ Marie Wingyee Lau,¹ Serena Perrotta²

¹*Department of Physics & Astronomy, University of California, Riverside, CA 92521, USA*

²*Center for Astrophysics and Space Sciences, University of California, San Diego, CA 92093, USA*

Accepted XXX. Received YYY; in original form ZZZ

ABSTRACT

Extremely Red Quasars (ERQs) are thought to represent a brief episode of young quasar and galactic evolution characterized by rapid outflows and obscured growth due to dusty environments. We use new redshift measurements from CO and Ly α emission-lines to better constrain outflow velocities from previous line measurements. We present sample of 82 ERQs, and the analysis confirms that ERQs have a higher incidence of large C IV blueshifts, accompanied by large Rest Equivalent Widths (REWs) and smaller line widths than blue quasars. We find that strong blueshifts ($>2000 \text{ km s}^{-1}$) are present in 12/54 (22.22%) of ERQs with the most robust redshift indicators. At least 4 out of 15 ERQs in the sample also have blueshifts in their H β and low-ionization UV lines ranging from -500 to -1500 km s^{-1} . ERQs with strong C IV blueshifts are substantially offset in C IV REW and Full-Width at Half-Maximum (FWHM) from typical blue quasars in the same velocity range. ERQs have average values of REW = 124Å and FWHM = 5274 km s^{-1} , while blue quasars have REW = 24Å and FWHM = 6973 km s^{-1} . The extreme nature of the outflows in ERQs might explain some of their other spectral properties, such as the large C IV REWs and peculiar wingless profiles owing to more extended broad-line regions participating in outflows. The physical reasons for the extreme outflow properties of ERQs are unclear; however, larger Eddington ratios and/or softer ionizing spectra incident on the outflow gas cannot be ruled out.

Key words: galaxies: active – quasars: emission lines – galaxies: intergalactic medium – galaxies: evolution – galaxies: high-redshift

1 INTRODUCTION

Quasars are supermassive black holes rapidly growing by accretion of infalling material at the center of their host galaxy. Accretion can coincide with streams of infalling gas, or galactic assembly, at high redshift. Merger activity, or infalling gas, may be the triggers supplying matter for starbursts and quasar activity (Hopkins et al. 2006, 2008; Somerville et al. 2008; Kereš et al. 2009; Dekel et al. 2009; Faucher-Giguère & Kereš 2011; Fumagalli et al. 2014; Glikman et al. 2015). This rapid accretion can coincide with outflows, generating feedback, and potentially influence the galaxy’s formation (Costa et al. 2014; Nelson et al. 2015; Suresh et al. 2019). A possible evolutionary scheme is where the central black hole initially grows in obscurity until feedback generates outflows, and clears the obscuring interstellar material, revealing a normal blue quasar (Sanders et al. 1988; Di Matteo et al. 2005; Hopkins et al. 2006, 2008, 2016; Rupke & Veilleux 2011, 2013; Liu et al. 2013; Stacey et al. 2022).

Red quasars are important for testing the hypothesis that obscured quasars may be in a young, and short-lived, phase in their evolution. Young quasars may be reddened by dust created in a major starburst inside the galaxies, triggered by a merger or cold-mode ac-

cretion. These reddened quasars may show signs of youth such as high accretion rates, more infall from the intergalactic medium, or powerful outflows, as they transform in to blue/unobscured quasars. Studies of red/obscured quasars have found many to be in mergers or high-accretion phases (Glikman et al. 2015; Wu et al. 2018; Zakamska et al. 2019).

Extremely red quasars (ERQs) are a unique quasar population selected from the Baryon Oscillation Spectroscopic Survey (BOSS, ?) in the Sloan Digital Sky Survey-III (SDSS, ?) and the ALL-WISE data release (??) of the Wide-field Infrared Survey Explorer (WISE, ?), based on red rest-UV to mid-IR colors, $i-W3 > 4.6$ (AB magnitudes Ross et al. 2015; Hamann et al. 2017). They are of particular interest because of a suite of other spectral properties connected to their extreme red colors, namely, unusually strong C IV $\lambda 1549$ emission lines with peculiar wingless profiles and frequent large blueshift, a high incidence of broad C IV outflow absorption lines, and exceptionally fast outflows measured in [O III] $\lambda 4959, 5007$ (Hamann et al. 2017; Perrotta et al. 2019). All of these features might be explained by exceptionally powerful accretion-disk outflows, e.g., that produce spatially-extended C IV broad emission line regions that produce large C IV rest equivalent widths (REWs) and feed into the fast, lower-density [O III] outflows farther out (Zakamska et al. 2016; Hamann et al. 2017; Perrotta et al. 2019). This evidence for prodigious outflows, combined with the extreme dust reddening, make

* E-mail: jgill016@ucr.edu

ERQs prime candidates for quasars driving feedback to their host galaxies during the early stages of massive galaxy evolution.

An essential ingredient for understanding quasar outflows, and the exotic properties of ERQs in particular, is accurate systemic redshifts to define the outflow speeds and kinetic energies. The most accurate redshift indicators are narrow emission lines, like [O III] $\lambda 5007$, that form in the extended galactic or circumgalactic environments of quasars. When these lines are not available, H β and various low-ionization broad emission lines in the UV, such as Mg II $\lambda 2800$, O I $\lambda 1304$, can be useful for normal quasars because they are less likely to be blueshifted (i.e., participating in outflows) than high-ionization emission lines like C IV (e.g. Shen et al. 2008; Shen et al. 2016; Li et al. 2017).

However, these redshift indicators are often problematic for ERQs because outflow signatures are more common and more extreme throughout their spectra. In particular, their [O III] lines are typically very broad and blueshifted with no distinct narrow components that might form in the extended/galactic environments (Zakamska et al. 2016; Perrotta et al. 2019), and their low-ionization broad emission lines often have large measurement uncertainties due to noisy spectra and they might be affected by large blueshifts/outflow speeds throughout the broad emission-line region (including more than just the high-ionization gas, see Section 3 below).

In this paper, we provide reliable systemic redshifts for a sample of 82 ERQs that have existing measurements of CO in their host galaxies (Hamann et al. 2023 in preparation) and/or narrow Ly α emission lines (Lau et al. 2022; Gillette et al. 2023, and this work) that form in their extended circumgalactic and/or halo environments. We then use these data to derive blueshifts/outflow speeds for the ERQ C IV $\lambda 1549$ broad emission lines and, whenever possible, reassess the [O III] $\lambda 5007$ outflow speeds reported previously by (Zakamska et al. 2016; Perrotta et al. 2019, and by Lau et al. in prep.). Our findings provide more accurate results, but support previous claims that ERQs have an unusually high frequency of fast/powerful outflows in these emission line regions, e.g., compared to normal blue quasars at similar redshifts and luminosities.

This paper is organized as follows. Section 2 describes selection criteria for quasars from catalog spectra and their redshifts. Section 3 describes our revised C IV and [O III] emission-line blueshifts and outflows. Section 4 discusses and summarizes correlations in measured parameters and emission features, such as blueshift, emission strength, and line width. Throughout this paper we adopt a Λ -CDM cosmology with $H_0 = 69.6 \text{ km s}^{-1} \text{ Mpc}^{-1}$, $\Omega_M = 0.286$ and $\Omega_\Lambda = 0.714$, as adopted by the online cosmology calculator developed by Wright (2006). All magnitudes are in the AB system. Reported wavelengths are in vacuum and in the heliocentric frame.

2 SAMPLE SELECTION & SYSTEMIC REDSHIFTS

The parent sample for our study is the 205 ERQs selected to have $i-W3 > 4.6$ in the combined BOSS survey Hamann et al. (2017). Those authors provide detailed data for the C IV emission lines, including velocity shifts relative to the BOSS DR12 catalogue redshifts (see their Appendix A). The DR12 redshifts derive from automated fits to the BOSS spectra, plus algorithmic corrections based on nominal line blueshifts, that can be off by hundreds or $>1000 \text{ km s}^{-1}$ for quasars like ERQs with unusual emission-line properties.

For the present study, we select ERQs from Hamann et al. (2017) that have other, more reliable measurements of the quasar systemic redshifts. These include 14 ERQs with ALMA sub-mm CO(4-3) emission-line measurements by Hamann et al. (2023 in prep.), 6

ERQs with KCWI (integrated field spectroscopy) of the extended Ly α halos by Gillette et al. (submitted), and 54 ERQs with narrow Ly α emission spikes in their BOSS spectra caused by halo emission. For some of our analysis, we also include 8 ERQs that have well-measured Mg II emission lines in their BOSS spectra, as measured by Gillette et al. (2023c in prep.).

Table 1 lists some basic catalogue properties and measurements for the total sample of 82 ERQs. The total ERQ sample has median color $i-W3 \approx 5.3$ and redshifts in the range $1.8 \leq z \leq 3.7$. The subsample of 20 ERQs with z_{best} from either CO or Ly α -halo has median color $i-W3 \approx 5.7$, while the 54 ERQs with only a Ly α -spike redshift have median color $i-W3 \approx 5.1$. The small color difference between these two subsamples can be attributed to two factors beyond counting statistics in the samples sizes: 1) our preference for redder ERQs in the ALMA CO and KCWI Ly α -halo observations, and 2) redder ERQs having fainter rest-UV fluxes that lead to noisier BOSS spectra and greater difficulty in identifying a narrow Ly α -spike for our study (Section 2).

We include a large comparison sample of 39,909 (mostly) blue quasars from the SDSS survey with systemic redshifts measured from the Mg II $\lambda 2800$ broad emission lines (Gillette et al. 2023c in prep.). Mg II provides reasonably accurate systemic redshifts for normal blue quasars. For example, Shen et al. (2008) report that, in a large sample of SDSS quasars, the Mg II line has average blueshift relative to [O III] of -97 km s^{-1} and a dispersion in the measured shifts of 269 km s^{-1} . The sample with Mg II measurements are from emission-line profile fitting to SDSS BOSS spectra, is done with similar methodology as described in Hamann et al. (2017), and with care taken to exclude bad data with custom signal-to-noise measurements and rejection criteria. Mg II emission is fit with a symmetric Gaussian or double-Gaussian profile, after the Fe II complex near Mg II is removed using a Fe II emission template. Details and results of the fitting in the blue quasar sample to will be presented in Gillette et al. (2023c in prep). C IV blueshifts are determined for the blue quasar sample by calculating the velocity shift of its centroid from the Mg II profile centroid.

2.1 Systemic Redshift Priorities

Some ERQs in our sample have available more than one of the systemic redshift indicators mentioned above. We choose a single value of z_{best} for each quasar based on the following priorities. The CO(4-3) emission line has highest priority because it forms (primarily) in dense molecular clouds inside the host galaxies. Although there can be gas motions within the galaxies, we expect the CO line centroids to have velocities similar to the central black holes/quasars (see Hamann et al. 2023 in prep. for discussion). Thus we adopt the CO line centroids provided by Hamann et al. (2023, in prep.), measured from spatially-integrated spectra, for z_{best} when available.

Second priority for z_{best} , if a CO(4-3) measurement is not available, is a narrow Ly α emission line arising from the spatially-resolved ERQ halo/circumgalactic medium (as measured from Keck-KCWI observations by Lau et al. 2022; Gillette et al. 2023). Redshifts determined this way are denoted by “Ly α -halo” in the z_{best} indicator column in Table 1. We specifically derive redshifts from the spatially-averaged Ly α emission from extended regions around the ERQs that exclude the central ~ 1 arcsecond diameter. Excluding the central regions is a precaution to avoid potential i) rapid gas flows near the galactic nucleus, and ii) Ly α absorption features appearing along direct sight lines toward the central quasar.

One important result from our studies of ERQ halos with Keck-KCWI (Lau et al. 2022; Gillette et al. 2023) was to confirm the spec-

Table 1. ERQ Sample Properties. z_{em} is from the SDSS DR12Q BOSS catalogue emission-line measurement. $W3$ magnitude, and $i-W2$ color are from WISE and BOSS. z_{best} is the best estimate of the reference systemic redshift based on either CO (from Hamann et al. 2023 in prep.), narrow Ly α emission lines in the extended ERQ halos (from Gillette et al. 2023), or narrow Ly α emission-line “spikes” as measured here (Section 2) from the BOSS spectra. C iv REW, Full-Width at Half-Maximum (FWHM), and Blueshifts are from emission-line profile fitting done in Hamann et al. (2017). [O III] λ 5007 emission blueshift measurements are from Perrotta et al. (2019), when available, and blueshifted from the reference systemic.

Notes. ^a ERQ’s BOSS spectra show strong Mg II or O I emission as well as having a CO or Ly α redshift indicator. ^b [O III] v_{98} blueshift determined from Keck-OSIRIS observations by Lau et al. (in prep.).

ERQ Name	z_{em}	W3 (mag)	$i-W3$ (mag)	z_{best}	z_{best} indicator	C iv REW (Å)	C iv FWHM (km s ⁻¹)	C iv shift (km s ⁻¹)	[O III] v_{98} (km s ⁻¹)
J000610.67+121501.2	2.3099	14.09	8.01	2.3183	CO	107	4540	-2260	-5959
J002400.67-081110.2	2.0633	16.19	4.63	2.0638	Mg II	53	2042	108	-
J005233.24-055653.5	2.3542	16.00	6.37	2.3631	CO	188	2451	-1469	-
J011601.43-050503.9	3.1825	15.53	6.24	3.1875	Ly α -Spike	94	2291	-1240	-
J015222.58+323152.7	2.7859	15.76	5.39	2.7925	Ly α -Spike	136	3677	-980	-
J022052.11+013711.1	3.1376	15.75	6.24	3.1375	Ly α -Halo	328	2613	-576	-
J080547.66+454159.0	2.3258	15.51	6.32	2.3127	Ly α -Spike	109	2667	-524	-4982
J082224.01+583932.8	2.5469	15.37	4.81	2.5667	Ly α -Spike	65	5474	-3246	-
J082536.31+200040.3	2.0938	16.77	4.74	2.0881	Ly α -Spike	211	3265	-473	-
J082653.42+054247.3	2.5734	15.18	6.01	2.5780	CO	205	2434	-369	-3420
J083200.20+161500.3	2.4472	14.98	6.74	2.4249	CO	300	3082	-297	-5258
J083448.48+015921.1	2.5942	14.86	5.99	2.5850	CO	209	2863	198	-4426
J084447.66+462338.7	2.2168	15.15	5.96	2.2226	Ly α -Spike	161	1656	-225	-
J085039.50+515831.0	1.8914	15.62	4.97	1.9003	Mg II	65	1145	-1062	-
J085229.65+524730.8	2.2674	16.48	4.74	2.2526	Ly α -Spike	64	1291	-322	-
J090014.07+532148.7	2.1098	17.00	7.31	2.1042	Mg II	47	4296	-756	-
J090306.18+234909.8	2.2635	16.91	5.02	2.2686	Mg II	144	2481	-372	-
J091303.90+234435.2	2.4195	16.41	5.31	2.4335	Ly α -Spike	145	2190	-448	-2099
J092049.59+282200.9	2.2959	15.95	4.83	2.2976	Ly α -Spike	197	1048	-99	-
J092604.08+524652.9	2.3467	17.13	4.71	2.3516	Ly α -Spike	86	3053	-634	-
J093638.41+101930.3	2.4531	15.42	6.17	2.4523	Ly α -Spike	172	1271	196	-
J095033.51+211729.1	2.7447	16.33	5.52	2.7430	Ly α -Spike	272	1387	86	-
J101326.23+611219.9	3.7028	15.17	5.91	3.7061	Ly α -Spike	281	5133	-2945	-
J101533.65+631752.6	2.2255	16.39	5.48	2.2337	Ly α -Spike	130	2012	-394	-
J102353.44+580004.9	2.5972	15.97	5.11	2.5996	Ly α -Spike	116	2107	-120	-
J104718.35+484433.8	2.2751	15.57	5.30	2.2767	Ly α -Spike	158	2521	-33	-
J104754.58+621300.5	2.5361	16.25	5.08	2.5566	Ly α -Spike	105	5081	-2382	-
J110202.68-000752.7	2.6261	17.05	4.87	2.6261	Ly α -Spike	121	3767	-311	-
J111346.10+185451.9	2.5160	17.07	4.62	2.5188	Ly α -Spike	127	986	-125	-
J111516.33+194950.4	2.7924	17.04	4.96	2.7989	Ly α -Spike	247	1739	-197	-
J111729.56+462331.2	2.1317	15.55	6.26	2.1309	Ly α -Spike	395	3053	-390	-
J112124.55+570529.6	2.3834	14.98	5.07	2.3885	Ly α -Spike	28	1780	-392	-
J113721.46+142728.8 ^a	2.3008	15.13	4.87	2.3025	CO	98	4734	-2158	-
J113834.68+473250.0 ^a	2.3105	15.85	6.09	2.3146	Ly α -Spike	177	3296	-1202	-3928
J113931.09+460614.3	1.8202	15.30	6.44	1.8182	Mg II	47	1239	110	-
J114508.00+574258.6	2.7904	14.27	4.84	2.8747	Ly α -Halo	38	9103	-8655	-
J121253.47+595801.2	2.5841	15.85	4.95	2.5619	Ly α -Spike	107	1402	181	-
J121704.70+023417.1	2.4163	15.43	5.59	2.4280	CO	181	2604	-850	-2640
J122000.68+064045.3	2.7963	16.57	4.88	2.7732	Ly α -Spike	113	1047	63	-
J123241.73+091209.3	2.3814	14.39	6.76	2.4050	CO	225	4787	-3526	-7026
J124106.97+295220.8	2.7935	16.49	5.35	2.7976	Ly α -Spike	138	2600	-1382	-
J124738.40+501517.7	2.3858	16.53	4.97	2.4014	Ly α -Spike	135	3268	-909	-
J125019.46+630638.6	2.4016	16.42	5.47	2.4049	Ly α -Spike	242	1881	0	-
J125944.55+240708.3	2.1660	16.04	4.60	2.1665	Mg II	46	4284	-115	-
J130114.46+131207.4	2.7867	16.26	5.11	2.7892	Ly α -Spike	186	1877	-347	-
J130630.66+584734.7	2.2970	16.71	5.01	2.2986	Ly α -Spike	331	1133	-30	-
J130936.14+560111.3	2.5687	15.47	6.45	2.5794	Ly α -Spike	161	3630	-519	-
J131047.78+322518.3	3.0168	15.05	5.26	3.0164	Ly α -Spike	226	2794	-914	-
J131330.67+625957.2	2.3681	17.50	4.67	2.3714	Ly α -Spike	82	1589	49	-
J131351.23+345405.3	1.9718	15.17	4.64	1.9706	Mg II	18	2397	-98	-
J131628.32+045316.2	2.1446	15.55	5.74	2.1598	CO	63	3010	-898	-
J131833.76+261746.9	2.2721	16.39	4.91	2.2746	Ly α -Spike	150	1280	-23	-
J132654.95-000530.1	3.3241	15.17	4.75	3.3068	Ly α -Spike	77	1607	-56	-

Table 1. ERQ Sample Properties (Continued)

ERQ Name	z_{em}	W3 (mag)	$i-W3$ (mag)	z_{best}	z_{best} indicator	C iv REW (Å)	C iv FWHM (km s ⁻¹)	C iv shift (km s ⁻¹)	[O III] v ₉₈ (km s ⁻¹)
J133611.79+404522.8	2.0793	14.10	6.51	2.0882	Mg II	20	6154	-2724	-
J134254.45+093059.3 ^a	2.3430	15.92	4.90	2.3470	CO	66	3246	-1558	-4779
J134417.34+445459.4	3.0359	15.54	6.78	3.0408	Ly α -Spike	310	2871	-1152	-
J134800.13-025006.4	2.2495	15.91	5.70	2.2374	CO	87	3654	-1059	-4221
J135557.60+144733.1 ^a	2.7037	15.71	4.71	2.6880	Ly α -Spike	118	2958	-252	-
J135608.32+073017.2	2.2691	16.52	5.08	2.2716	Ly α -Spike	110	2043	117	-1767
J143159.76+173032.6	2.3765	16.02	5.82	2.3880	Ly α -Spike	177	2084	-170	-
J143853.61+371035.3	2.3931	15.81	5.50	2.3981	Mg II	29	3115	-137	-
J144932.66+235437.2	2.3428	16.79	4.73	2.3453	Ly α -Spike	98	1352	95	-
J145113.61+013234.1	2.7734	14.77	5.67	2.8130	Ly α -Halo	87	6231	-3376	-
J145148.01+233845.4	2.6214	15.01	5.51	2.6348	Ly α -Halo	89	4166	-3040	-
J150117.07+231730.9	3.0254	16.20	5.90	3.0204	Ly α -Spike	231	4035	-1940	-
J152941.01+464517.6	2.4201	15.92	4.82	2.4189	Ly α -Spike	159	1896	151	-
J153108.10+213725.1	2.5689	16.92	5.23	2.5639	Ly α -Spike	213	2767	-253	-
J153446.26+515933.8	2.2650	17.01	4.73	2.2658	Ly α -Spike	127	1156	95	-
J154243.87+102001.5	3.2150	15.62	6.58	3.2166	Ly α -Spike	114	3901	-2303	-
J154743.78+615431.1	2.8682	16.81	4.89	2.8674	Ly α -Spike	128	1177	10	-
J154831.92+311951.4	2.7364	16.91	4.82	2.7462	Ly α -Spike	127	3050	-1151	-
J155725.27+260252.7	2.8201	16.91	4.92	2.8217	Ly α -Spike	56	1182	-1	-
J164725.72+522948.6	2.7193	16.40	5.23	2.7206	Ly α -Spike	124	1905	-29	-
J165202.64+172852.3	2.9425	14.91	5.39	2.9548	Ly α -Halo	125	2403	-1285	-2534
J170558.64+273624.7	2.4483	15.48	5.13	2.4461	Ly α -Halo	157	1301	267	-
J171420.38+414815.7	2.3419	16.65	4.70	2.3303	Ly α -Spike	130	3816	-816	-
J211329.61+001841.7	1.9961	16.08	7.05	1.9998	Ly α -Spike	171	1565	-226	-
J220337.79+121955.3	2.6229	15.50	6.21	2.6229	Ly α -Spike	266	1070	110	-
J221524.00-005643.8	2.5086	16.06	6.17	2.5093	CO	153	4280	-1394	-3877
J222307.12+085701.7 ^a	2.2890	15.65	5.60	2.2902	CO	77	3661	-1130	-7760 ^b
J223754.52+065026.6	2.6088	16.17	5.79	2.6117	Ly α -Spike	141	1391	-11	-
J232326.17-010033.1	2.3561	15.22	7.19	2.3805	CO	256	3989	-2756	-6458

ulation by Hamann et al. (2017) that the narrow Ly α emission spikes seen (with surprising frequency) in aperture spectra of ERQs form in their inner halos. In particular, the narrow Ly α spikes in aperture spectra consistently have profiles and redshifts very similar to the spatially-resolved halo emission in the KCWI data.

Our third priority for z_{best} values, when neither CO nor spatially-resolved Ly α data are available, are a narrow Ly α spike in aperture spectra of the ERQs. Lau et al. (2022) discussed ERQ J000610+121501 is a good example, where a distinct narrow Ly α spike in aperture spectra clearly forms in the inner halo, and confirmed by mapping data from Keck-KCWI. Gillette et al. (2023) discusses a wider range of cases, and include some where aperture spectra show the profile of narrow Ly α spike emitted from the halo blends smoothly into the broad Ly α emission line of the quasar. We selected the 59 ERQs from Hamann et al. (2017) with Ly α spikes attributable to halo emission based on the appearance of a single narrow emission peak with FWHM < 1,000 km s⁻¹ that is well-measured above the noise and shows no indications of overlying Ly α absorption that might distort the emission spike profile. The centroids of these spikes provide z_{best} . Although we give these z_{best} values a lower priority than estimates from spatially-resolved Ly α halo data, their typical uncertainties are $\leq \sim 200$ km s⁻¹ based on both the line measurement accuracies and our experience comparing these Ly α spikes to spatially-resolved Ly α emission from ERQ halos (Lau et al. 2022; Gillette et al. 2023). Quasars with z_{best} determined this way are denoted by “Ly α -spike” in Table 1.

Lowest priority are the eight ERQs with z_{best} measurements from their low-ionization Mg II $\lambda 2800$ broad emission lines (from a large

general study of quasar emission-line blueshifts by Gillette et al. 2023c in prep.). We consider these to be the least reliable redshifts because, unlike normal blue quasars, the low-ionization emission lines in ERQs can also be involved fast outflows leading to large blueshifts (see Hamann et al. 2018, also Section 4 below). None of these quasars with well-measured Mg II lines also have CO or Ly α measures. We note five quasars with CO, or Ly α , redshifts and also low-ionization lines with have visibly obvious peak/centroids in Mg II or O I $\lambda 1304$, indicated in Table 1.

2.2 Potential Biases

Before discussing emission blueshifts, we consider potential biases in the properties of our ERQ subsamples. The ALMA CO and KCWI Ly α -halo observations both tended to favor ERQs with large C iv REWs (≥ 100 Å) and relatively broad C iv profiles (FWHM ≥ 2000 km s⁻¹). This represents the majority of ERQs having exotic spectral line/outflow properties (Section 1 of Hamann et al. 2017; Perrotta et al. 2019). We also tried to include sources with the reddest $i-W3$ colors among ERQs. Altogether, however, these samples span a wide range of ERQs because we wanted to examine a range, and because observational constraints tended to randomize the samples with respect to C iv properties (e.g., source brightness limits, scheduling constraints, and requirements for low declinations and a very narrow redshift range (near ~ 2.4) for the ALMA CO observations). Therefore, while these samples do intentionally include some of the most extreme ERQs, e.g., J123241+091209 and J232326-010033 with fast [O III] outflows (Zakamska et al. 2016; Perrotta et al. 2019)

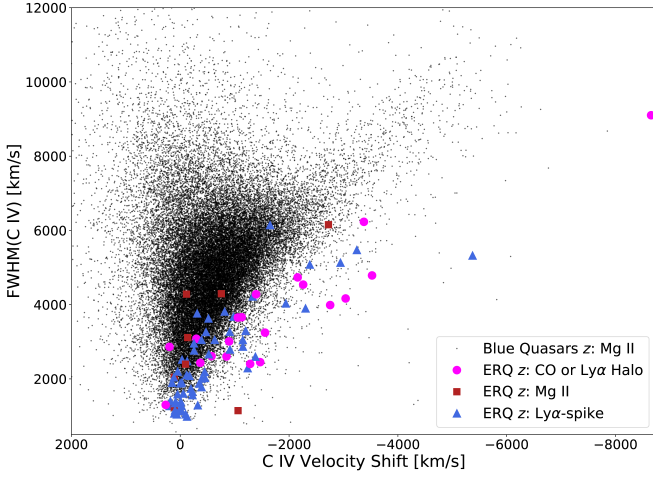


Figure 1. C IV FWHM vs velocity shift of ERQs with the best systemic redshift estimations and blue quasars. Pink dots indicates ERQs with systemic redshift estimates from either CO from ALMA or Ly α Halo from KCWI, red squares for ERQ redshifts estimates with Mg II from BOSS, and blue triangles for ERQ redshifts estimates from narrow Ly α from BOSS.

and J114508+574258 with a previously-known large C IV blueshift (Hamann et al. 2017), they should be overall approximately representative of the majority of ERQs with $\text{FWHM}(\text{C IV}) \geq 2000 \text{ km s}^{-1}$. We also note that any remaining tendency for large C IV REWs in these sample might, if anything, favor small C IV blueshifts because large C IV REWs are known to correlate strongly with small blueshifts in the general quasar population (Richards et al. 2011; Coatman et al. 2016, 2019; Rankine et al. 2020; Temple et al. 2023, Gillette et al. 2023c in prep., also Section 3.1).

There is, however, a substantial bias in the sample of 59 ERQs selected to have a narrow Ly α spike in their BOSS spectra. There are two reasons for this. First, selecting for a narrow spike in Ly α strongly favors ERQs whose entire Ly α profile is narrow and whose other “broad” emission lines, including C IV $\lambda 1549$, are also unusually narrow (e.g., compared to the average for ERQs). Second, narrow C IV emission lines correlate strongly with smaller C IV blueshifts (Figure 1, also Richards et al. 2011; Coatman et al. 2016, 2019; Rankine et al. 2020; Temple et al. 2023, and Gillette et al. 2023c in prep.). The net effect is that this sample is biased towards both narrower C IV lines and smaller C IV blueshifts than the general ERQ population (see Section 2.2 for more discussion).

3 EMISSION-LINE BLUESHIFTS & OUTFLOW SPEEDS

3.1 C IV Blueshifts

Table 1 lists C IV blueshifts relative to z_{best} for every ERQ in our sample. We use the C IV emission-line wavelengths preferred by Hamann et al. (2017), namely, the midpoint in the fitted line profiles at their half-maximum heights, and a rest wavelength equal to the average for the doublet, 1549Å. Midpoint wavelengths are the same as the centroid for symmetric profiles, but they avoid possible asymmetries, blueshifted absorption or noise problems in the line wings that would affect the centroid values.

Figures 1 and 2 plot the C IV blueshifts versus $\text{FWHM}(\text{C IV})$ and $\text{REW}(\text{C IV})$, respectively, for ERQs compared to the normal blue quasar sample (Section 2). Notice that the “Ly α -spike” sample of ERQs strongly favors narrow C IV emission lines (Figure 1). This is not representative of the ERQs overall in (Hamann et al. 2017,

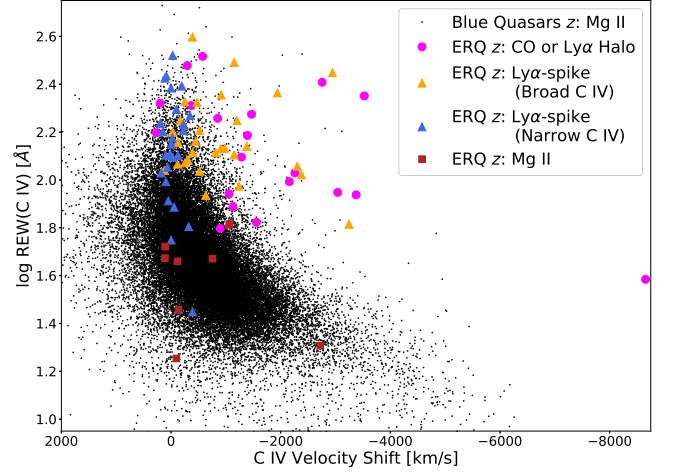


Figure 2. C IV REW vs velocity shift of ERQs with the best systemic redshift estimations and blue quasars. We use the same notation as Figure 1, except we separate the group with Ly α -spike measurements in to a broad-C IV ($\text{FWHM} \geq 2000 \text{ km s}^{-1}$) and narrow-C IV ($\text{FWHM} < 2000 \text{ km s}^{-1}$). Broad-C IV ERQs can show strongly blueshifted emission, while the narrow-C IV ERQs are typically more weakly blueshifted.

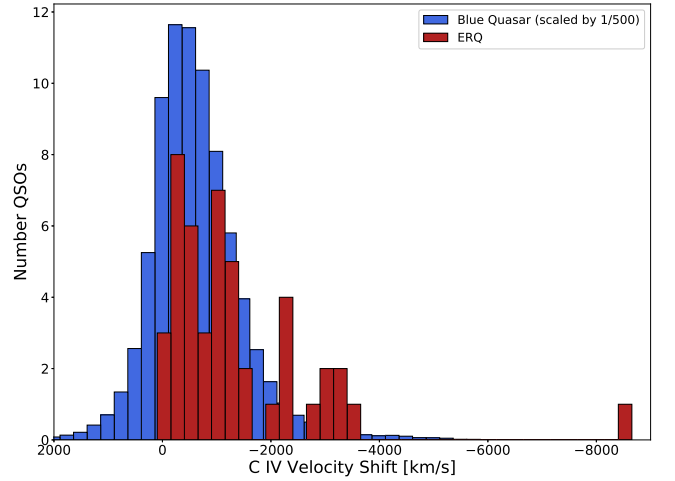


Figure 3. C IV velocity shifts for blue quasars and all ERQs that have reliable systemic redshift estimations from CO or Ly α , but excluding ERQs with narrow C IV profiles. We scale the much larger blue quasar distribution to compare with our sample. ERQs have a much higher fraction of high velocity C IV blueshifts than the normal blue quasar population.

see also Section 2). However, if we consider only sources with $\text{FWHM}(\text{C IV}) \geq 2000 \text{ km s}^{-1}$ in the Ly α -spike sample (orange triangles in Figure 2), the distribution of C IV blueshifts in that sub-sample, and its behavior in the 3-dimensional space that includes $\text{FWHM}(\text{C IV})$ and $\text{REW}(\text{C IV})$, closely resemble the ERQs in the CO and Ly α -halo samples (which all have $\text{FWHM}(\text{C IV}) \geq 2000 \text{ km s}^{-1}$).

Figure 3 and 4 compare the C IV blueshift and REW distributions, respectively, of ERQs to the blue quasar sample. The ERQs in these figures are from the combined sample of 74 sources with z_{best} from either CO, Ly α -halo, or a Ly α -spike with the additional constraint $\text{FWHM}(\text{C IV}) \geq 2000 \text{ km s}^{-1}$.

We can see from these figures that ERQs stand out from normal/blue quasars in several ways. First, ERQs have large C IV blueshifts at much larger $\text{REW}(\text{C IV})$ and somewhat smaller

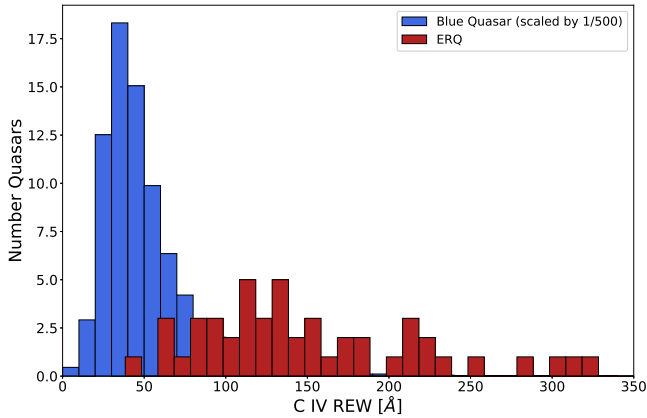


Figure 4. C IV REW for blue quasars and all ERQs that have reliable systemic redshift estimations from CO or Ly α , but excluding ERQs with narrow C IV profiles. We scale the much larger blue quasar distribution to compare with our sample. ERQs have considerably larger C IV REW than the normal blue quasar population.

FWHM(C IV) than normal blue quasars (Figures 2 and 1, respectively). It is well known that large C IV blueshifts correlate strongly with small C IV REWs (Figure 2) and large FWHMs (Figure 1) in normal blue quasars (Richards et al. 2011; Coatman et al. 2016, 2019; Rankine et al. 2020; Temple et al. 2020, 2023, Gillette et al. 2023c in prep.). The ERQs behave differently. They also exhibit a trend for larger blueshifts tied to larger FWHMs (seen in Figure 1) but, for any given blueshift, the ERQ population is offset toward smaller FWHMs. J114508+574258 is the ERQ with the largest C IV blueshift, at -8655 km s^{-1} (Table 1), and has one of the smallest C IV REWs and largest FWHMs among all ERQs (Hamann et al. 2017). These properties are consistent the direction of the trends in blue quasars. However, the C IV line in J114508+574258 is substantially broader and at least 4 times larger in REW than expected from trends in blue quasars (Figures 1 and 2). The ERQ samples overall are dramatically offset toward larger REWs than blue quasars, especially at large blueshifts. For example, for quasars with C IV blueshifts $>2000 \text{ km s}^{-1}$, the average REW among ERQs is 124 \AA compared to only 24 \AA for the blue quasar sample.

Another important difference is the larger fraction of ERQs with large blueshifts compared to the blue quasar population (Figure 3). For example, if we consider all ERQs with well-measured z_{best} in our study (excluding only those based on Mg II), the fraction with blueshifts $\geq 2000 \text{ km s}^{-1}$ is 12 out of 82, or 14.63 percent per cent. If we further exclude sources with $\text{FWHM}(\text{C IV}) < 2000 \text{ km s}^{-1}$ from our Ly α -spike sample, to be more representative of the majority of ERQs in Hamann et al. (2017), we find that 12 out of 54 (22.22 per cent) have blueshifts $>2000 \text{ km s}^{-1}$. In contrast, only 0.23 per cent of the 39909 blue quasars in our comparison sample have blueshifts in this range. Richards et al. (2011) find a similar number, with only 21 (0.13 per cent) out of 15,779 quasars having blueshift $\geq 2000 \text{ km s}^{-1}$ in their SDSS sample.

3.2 Revised [O III] Outflow Speeds

Table 1 provides recomputed [O III] outflow velocities, v_{98} when available, using our improved systemic redshifts. The [O III] data are from Perrotta et al. (2019) except for one quasar, J222307+085701, for which we present an [O III] measurement for the first time (from Lau et al. in prep.). Systemic redshifts used previously by

Perrotta et al. (2019) are based on the best redshift indicator available at that time, namely, either H β , low-ionization UV emission lines, or distinct narrow components in the [O III] (see their Table 1). Although not discussed explicitly by those authors, a few of the redshifts based on “low-ions” also considered a narrow core in the Ly α emission line, if one was present, similar to our analysis in Section 2.

Out of 15 ERQs with [O III] data from Perrotta et al. (2019) in our samples, 10 have revised redshifts different from the previous values by $\leq 200 \text{ km s}^{-1}$. This is generally good agreement for the purpose of studying high-speed quasar outflows. However, 4 have larger revised redshifts by $\geq 500 \text{ km s}^{-1}$ and 3 of those have larger revised redshifts by $\geq 1000 \text{ km s}^{-1}$. This implies substantially larger outflow speeds than the previous estimates. In the 4 ERQs with the largest changes, the [O III] v_{98} values jumped from -2034 to -2534 km s^{-1} in J165202+172852, from -5480 to -6458 km s^{-1} in J232326-010033, from -2872 to -3877 km s^{-1} in J221524-005643, and from -5580 to -7026 km s^{-1} in J123241+091209 (cf. Table 1 here and Table 4 in Perrotta et al. 2019). All 4 of these ERQs with the largest shifts do not have narrow emission features in the quasar spectra, such that the previous redshift estimates came from H β or low-ionization UV emission lines.

Five quasars with CO, or Ly α , redshifts and low-ionization lines with have visibly obvious peak/centroids in Mg II or O I. We measure velocity shifts of these low-ionization lines with respect to the most reliable emission lines available. These ERQs include J113721+142728, J113834+473250, J134254+093059, J135557+144733, and J222307+085701, with respective relative velocities of -218 , -62 , 145 , 278 , and -285 km s^{-1} . We discuss implications of these velocity shifts in Section 4.

One ERQ in our study with [O III] data from Perrotta et al. (2019), J083448+015921, has a revised redshift that is lower by 653 km s^{-1} . This revision changes the v_{98} estimate from -5079 km s^{-1} in Perrotta et al. (2019) to -4426 km s^{-1} here. This is surprising because both the CO(4-3) emission line and the low-ionization UV lines in the quasar spectrum, notably O I $\lambda 1304$, appear reasonably strong and well-measured. Perrotta et al. (2019) do not provide uncertainties on their redshift estimates, but a visual inspection suggests that they should be $< 200 \text{ km s}^{-1}$ (at 3σ). The formal uncertainty in the CO measurement by Hamann et al. (2023 in prep.) is 7.3 km s^{-1} . It seems unlikely that the redshift difference is caused by infall in the low-ionization broad emission lines relative to the quasar. We conclude that it might be due to a real kinematic offset between the quasar and the molecular gas emitting CO(4-3) in the quasar’s host galaxy.

4 SUMMARY & DISCUSSION

We present a sample of 82 ERQs that have improved estimates for redshift in order to better constrain outflow velocities from comparisons to previous line measurements. These comparisons are subject to selection biases (see Section 2.2), but overall we confirm ERQs have a higher incidence of large C IV blueshifts accompanied by large REWs and smaller line widths than blue quasars. Blueshifts $>2000 \text{ km s}^{-1}$ are present in 12/54 (22.22 per cent) of ERQs with the most robust z indicators. ERQs with blueshifts $>2000 \text{ km s}^{-1}$ are substantially offset in C IV REW and FWHM from typical blue quasars in the same velocity range, with ERQ averages of $\text{REW} = 124 \text{ \AA}$ and $\text{FWHM} = 5274 \text{ km s}^{-1}$, compared to blue quasar averages $\text{REW} = 24 \text{ \AA}$ and $\text{FWHM} = 6973 \text{ km s}^{-1}$.

Our systemic redshifts compared to the previous estimates by

Perrotta et al. (2019) already identifies 4 out of 15 ERQs in our sample with blueshifts in their H β and low-ionization UV lines ranging from -500 to -1500 km s $^{-1}$. This is a lower limit to the true fraction of ERQs with large blueshifts in these lines because some of the estimates in Perrotta et al. (2019) relied on narrow emission spikes in [O III], which agree well with our redshift estimates because they also form in extended environments around the quasars. Thus it appears that a significant fraction of ERQs have large blueshifts throughout their broad emission-line regions. This property of ERQs differs from the situation in normal blue quasars, where fast outflows in the broad emission-line regions are both much rarer than ERQs and primarily limited to the high-ionization gas emissions (e.g., C IV, Richards et al. 2011; Coatman et al. 2019; Rankine et al. 2020).

The extreme nature of the outflows in ERQs might explain some of their other spectral properties, such as the large C IV REWs, e.g., owing to more extended broad emission-line regions that have larger covering factors and reprocess more continuum light from the central quasars, and their peculiar wingless C IV profiles, e.g., if they form mostly in outflows instead of virialized gas near the inner accretion disk (Hamann et al. 2017). It is also interesting to consider that the exceptionally fast [O III] winds in ERQs might be an outer, lower-density extension to the broad emission-line outflows.

It remains unclear why ERQs tend to have faster/more powerful outflows than normal blue quasars, but there are two factors that might contribute. One is higher Eddington ratios, which can provide a greater radiative driving force compared to gravity. Another is softer UV continuum, where the weaker far-UV flux helps to maintain moderate ionization levels and substantial opacities in the outflow for radiative driving to be seen in the near-UV. There is strong observational evidence for both of these factors leading to faster outflows in normal blue quasars. For example, the He II $\lambda 1640$ emission-line REW roughly measures the ionizing flux at energies $h\nu > 54$ eV relative to the near-UV continuum, on which the line sits, inversely correlates with larger C IV emission-line blueshifts (Richards et al. 2011; Rankine et al. 2020; Temple et al. 2023, Gillette et al. 2023c in prep.) and faster C IV broad absorption-line (BAL) outflows (Baskin et al. 2013; Hamann et al. 2018; Rankine et al. 2020). This inverse relation is consistent with softer UV spectra playing an important role in outflows, and is indicated in hyper-luminous blue quasars (Vietri, G. et al. 2018). It has been shown that larger Eddington ratios can also correlate with larger C IV blueshifts (Baskin & Laor 2005; Coatman et al. 2016; Rankine et al. 2020; Temple et al. 2023, Gillette et al. 2023c in prep.).

More work is needed to determine if these trends also apply to ERQs and, moreover, if their extreme outflows result from them being at an extreme end of the trends found in blue quasars (e.g., with larger Eddington ratios or softer UV continua). Previous studies have found no significant trend in [O III] outflow speed with Eddington ratio (as measured from H β) among ERQs (see Figure 7 in Perrotta et al. 2019). Unfortunately, there are unique obstacles to testing these trends for ERQs. One is that their emission-line REWs are anomalously large, and He II is at least partly involved in that tendency (see Figure 8 in Hamann et al. 2017), which could confuse the relationship of this line with larger C IV blueshifts. Another challenge is that Eddington ratios require black hole mass estimates, which are derived normally from one of the broad emission lines like Mg II. We have shown above that ERQ lines like Mg II could have kinematics dominated by outflows, instead of virial motions in the local gravity, and thus making them unreliable for black hole mass determinations. Furthermore, obtaining bolometric luminosities necessary for Eddington ratios poses a greater challenge for ERQs compared to normal blue quasars, because their intrinsic SEDs are

potentially atypical. Nonetheless, we confirm the extreme properties of ERQ outflows, which motivates future efforts to understand what is the cause of their extreme nature and potential impacts on the host galaxy.

ACKNOWLEDGEMENTS

JG, FH, and MWL acknowledge support from the USA National Science Foundation grant AST-1911066. The data presented herein were obtained at the W. M. Keck Observatory, which is operated as a scientific partnership among the California Institute of Technology, the University of California and the National Aeronautics and Space Administration. The Observatory was made possible by the generous financial support of the W. M. Keck Foundation. Data presented herein were partially obtained using the California Institute of Technology Remote Observing Facility. The authors wish to recognize and acknowledge the very significant cultural role and reverence that the summit of Maunakea has always had within the indigenous Hawaiian community. We are most fortunate to have the opportunity to conduct observations from this mountain.

DATA AVAILABILITY

The data are available upon request.

REFERENCES

- Baskin A., Laor A., 2005, *Monthly Notices of the Royal Astronomical Society*, 356, 1029
- Baskin A., Laor A., Hamann F., 2013, *Monthly Notices of the Royal Astronomical Society*, 432, 1525
- Coatman L., Hewett P. C., Banerji M., Richards G. T., 2016, *Monthly Notices of the Royal Astronomical Society*, 461, 647
- Coatman L., Hewett P. C., Banerji M., Richards G. T., Hennawi J. F., Prochaska J. X., 2019, *Monthly Notices of the Royal Astronomical Society*, 486, 5335
- Costa T., Sijacki D., Haehnelt M. G., 2014, *MNRAS*, 444, 2355
- Dekel A., et al., 2009, *Nature*, 457, 451
- Di Matteo T., Springel V., Hernquist L., 2005, *Nature*, 433, 604
- Faucher-Giguère C.-A., Kereš D., 2011, *MNRAS*, 412, L118
- Fumagalli M., Hennawi J. F., Prochaska J. X., Kasen D., Dekel A., Ceverino D., Primack J., 2014, *ApJ*, 780, 74
- Gillette J., Lau M. W., Hamann F., Perrotta S., Rupke D. S. N., Wylezalek D., Zakamska N. L., Vayner A., 2023, Compact and Quiescent Circumgalactic Medium and Ly α Halos around Extremely Red Quasars (ERQs) ([arXiv:2303.12835](https://arxiv.org/abs/2303.12835))
- Glikman E., Simmons B., Maily M., Schawinski K., Urry C. M., Lacy M., 2015, *The Astrophysical Journal*, 806, 218
- Hamann F., et al., 2017, *MNRAS*, 464, 3431
- Hamann F., Herbst H., Paris I., Capellupo D., 2018, *Monthly Notices of the Royal Astronomical Society*, 483, 1808
- Hopkins P. F., Hernquist L., Cox T. J., Di Matteo T., Robertson B., Springel V., 2006, *ApJS*, 163, 1
- Hopkins P. F., Hernquist L., Cox T. J., Kereš D., 2008, *The Astrophysical Journal Supplement Series*, 175, 356
- Hopkins P. F., Torrey P., Faucher-Giguère C.-A., Quataert E., Murray N., 2016, *Monthly Notices of the Royal Astronomical Society*, 458, 816
- Kereš D., Katz N., Fardal M., Davé R., Weinberg D. H., 2009, *MNRAS*, 395, 160
- Lau M. W., Hamann F., Gillette J., Perrotta S., Rupke D. S. N., Wylezalek D., Zakamska N. L., 2022, *Monthly Notices of the Royal Astronomical Society*, 515, 1624
- Li J., et al., 2017, *The Astrophysical Journal*, 846, 79

- Liu G., Zakamska N. L., Greene J. E., Nesvadba N. P. H., Liu X., 2013, *MNRAS*, **436**, 2576
- Nelson D., Genel S., Vogelsberger M., Springel V., Sijacki D., Torrey P., Hernquist L., 2015, *MNRAS*, **448**, 59
- Perrotta S., Hamann F., Zakamska N. L., Alexandroff R. M., Rupke D., Wylezalek D., 2019, *MNRAS*, **488**, 4126
- Rankine A. L., Hewett P. C., Banerji M., Richards G. T., 2020, *Monthly Notices of the Royal Astronomical Society*, 492, 4553
- Richards G. T., et al., 2011, *The Astronomical Journal*, 141, 167
- Ross N. P., et al., 2015, *MNRAS*, **453**, 3932
- Rupke D. S. N., Veilleux S., 2011, *ApJ*, **729**, L27
- Rupke D. S. N., Veilleux S., 2013, *ApJ*, **768**, 75
- Sanders D. B., Soifer B. T., Elias J. H., Neugebauer G., Matthews K., 1988, *ApJ*, **328**, L35
- Shen Y., Greene J. E., Strauss M. A., Richards G. T., Schneider D. P., 2008, *The Astrophysical Journal*, 680, 169
- Shen Y., et al., 2016, *ApJ*, **831**, 7
- Somerville R. S., Hopkins P. F., Cox T. J., Robertson B. E., Hernquist L., 2008, *Monthly Notices of the Royal Astronomical Society*, 391, 481
- Stacey H. R., Costa T., McKean J. P., Sharon C. E., Rivera G. C., Glikman E., van der Werf P. P., 2022, *Monthly Notices of the Royal Astronomical Society*
- Suresh J., Nelson D., Genel S., Rubin K. H. R., Hernquist L., 2019, *MNRAS*, **483**, 4040
- Temple M. J., Banerji M., Hewett P. C., Rankine A. L., Richards G. T., 2020, *Monthly Notices of the Royal Astronomical Society*, 501, 3061
- Temple M. J., et al., 2023, Testing AGN outflow and accretion models with CIV and HeII emission line demographics in z=2 quasars ([arXiv:2301.02675](https://arxiv.org/abs/2301.02675))
- Vietri, G. et al., 2018, *A&A*, 617, A81
- Wright E. L., 2006, *PASP*, **118**, 1711
- Wu J., et al., 2018, *ApJ*, **852**, 96
- Zakamska N. L., et al., 2016, *MNRAS*, **459**, 3144
- Zakamska N. L., et al., 2019, *Monthly Notices of the Royal Astronomical Society*, 489, 497

This paper has been typeset from a $\text{\TeX}/\text{\LaTeX}$ file prepared by the author.